High-resolution mapping and modeling of anammox recovery from recurrent oxygen exposure

Accepted Manuscript

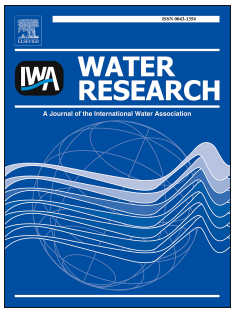

High-resolution mapping and modeling of anammox recovery from recurrent oxygen exposure

D. Seuntjens, J.M. Carvajal-Arroyo, M. Ruopp, P. Bunse, C.P. De Mulder, S. Lochmatter, S. Agrawal, N. Boon, S. Lackner, S.E. Vlaeminck

PII: S0043-1354(18)30563-3

DOI: 10.1016/j.watres.2018.07.024

Reference: WR 13923

To appear in: *Water Research*

Received Date: 17 November 2017

Revised Date: 3 July 2018

Accepted Date: 8 July 2018

Please cite this article as: Seuntjens, D., Carvajal-Arroyo, J.M., Ruopp, M., Bunse, P., De Mulder, C.P., Lochmatter, S., Agrawal, S., Boon, N., Lackner, S., Vlaeminck, S.E., High-resolution mapping and modeling of anammox recovery from recurrent oxygen exposure, *Water Research* (2018), doi: 10.1016/j.watres.2018.07.024.

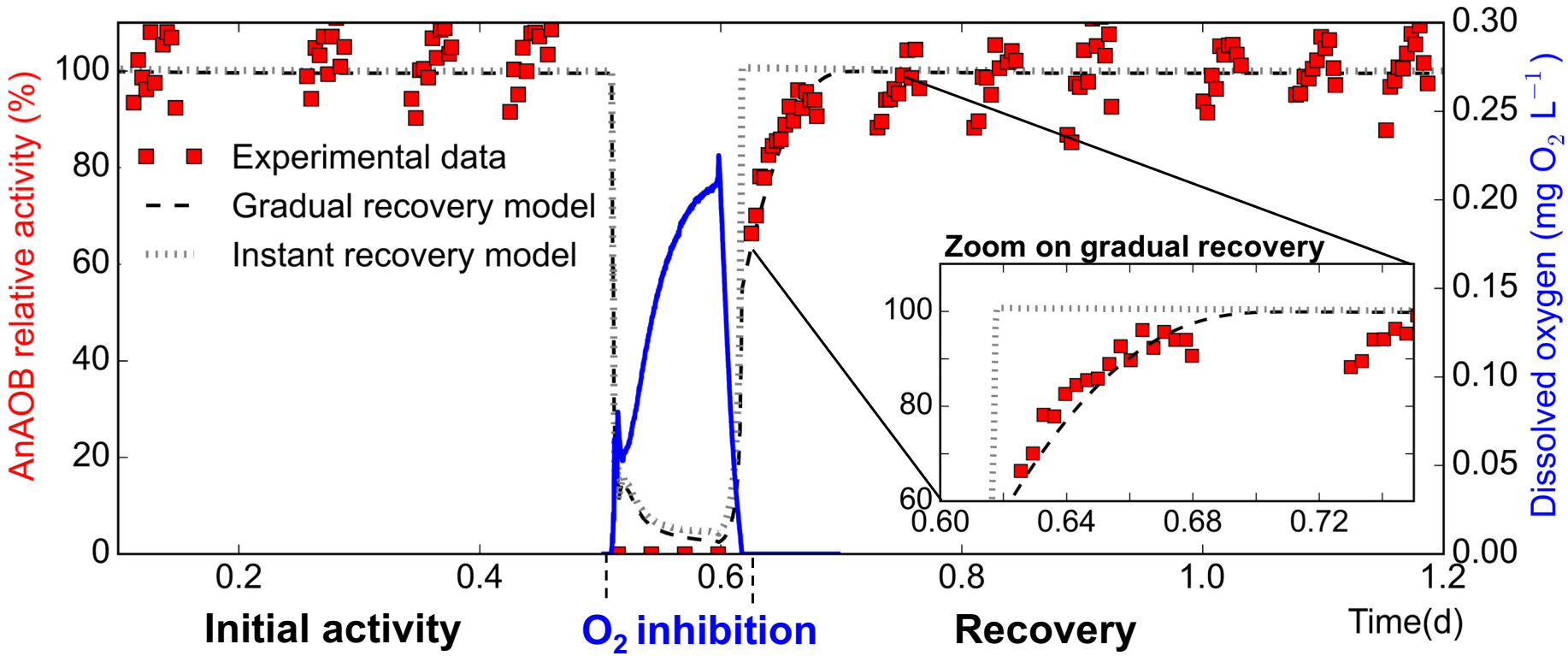
AnAOB relative activity (%)
Dissolved oxygen (mg O_2 L^{-1})
Experimental data
Gradual recovery model
Instant recovery model
Zoom on gradual recovery
Initial activity
O_2 inhibition
Recovery
Time(d)

High-resolution mapping and modeling of anammox recovery from recurrent oxygen exposure

Seuntjens D.[1], Carvajal-Arroyo J.M.[1], Ruopp M.[2], Bunse P.[2], De Mulder C.P.[3], Lochmatter S.[1], Agrawal S.[2], Boon N.[1], Lackner S.[2,§] and Vlaeminck S.E.[1,4,§,*]

[1] Center for Microbial Ecology and Technology (CMET), Ghent University, Gent, Belgium

[2] Technische Universität Darmstadt, Institute IWAR, Chair of Wastewater Engineering, Darmstadt, Germany

[3] Biomath, Ghent University, Gent, Belgium

[4] Research group of Sustainable Energy, Air and Water Technology, University of Antwerp, Antwerpen, Belgium

[§] Equal contribution as senior authors

[*] Corresponding author: siegfried.vlaeminck@uantwerpen.be

Keywords

Monod, partial nitritation/anammox, inhibition, intermittent aeration, energy-positive, sewage treatment

Abstract

Oxygen inhibits anammox, a bioconversion executed by anoxic ammonium oxidizing bacteria (AnAOB). Nonetheless, oxygen is mostly found in the proximity of AnAOB in nitrogen removal applications, being a substrate for nitritation. The experiments performed to date were mostly limited to batch activity tests where AnAOB activity is estimated during oxygen exposure. However, little attention has been paid to the recovery and reversibility of activity following aerobic conditions, of direct relevance for bioreactor operation. In this work, anoxic and autotrophic reactor cultivation at 20°C yielded an enriched microbial community in AnAOB, consisting for 75% of a member of the genus *Brocadia*. High-resolution kinetic data were obtained with online ammonium measurements and further processed with a newly developed Python data pipeline. The experimentally obtained AnAOB response showed complete inhibition until micro-aerobic conditions were reached again (<0.02 mg O_2 L^{-1}). After oxygen inhibition, AnAOB recovered gradually, with recovery times of 5-37h to reach a steady-state activity, dependent on the perceived inhibition. The recovery immediately after inhibition was lowest when exposed to higher oxygen concentrations (range: 0.5-8 mg O_2 L^{-1}) with long contact times (range: 9-24h). The experimental data did not fit well with a conventional 'instant recovery' Monod-type inhibition model. Yet, the fit greatly improved by incorporating a dynamic growth rate formula accurately describing gradual activity recovery. With the upgraded model, long-term kinetic simulations for partial nitritation/anammox (PN/A) with intermittent aeration showed a decrease in growth rate compared to the instant recovery mode. These results indicate that recovery of AnAOB

38 after oxygen exposure was previously overlooked. It is recommended to account for this
39 effect in the intensification of partial nitritation/anammox.

1. Introduction

Oxygen inhibits anoxic ammonium oxidation (anammox), a bioconversion executed by anoxic ammonium oxidizing bacteria (AnAOB). Nonetheless, oxygen is mostly found in their cell-proximity in biotechnological applications. Partial nitritation/anammox (PN/A) is a most cost-effective technology to remove ammonium from wastewater autotrophically, i.e. without organic carbon, producing mainly nitrogen gas and some nitrate It is already successfully implemented to treat ammonium-rich streams (500-1000 mg N L^{-1}) at higher temperatures (30-35°C), as the so-called sidestream PN/A process treating reject water from digested sewage sludge (Lackner et al., 2014). The so-called mainstream application of PN/A is in the waterline of a sewage treatment plant, following a carbon-removal step. This approach is less mature, yet of high interest, is it can enable treatment facilities to become a net producer (rather than consumer) of electricity (Verstraete & Vlaeminck, 2011). Specific challenges for mainstream PN/A relate to its lower temperatures (8-25°C in central Europe), lower influent ammonium concentrations (30-50 mg N L^{-1}) and higher levels of organics (e.g. biodegradable COD/N around 2). Agrawal et al. (2018) recently proposed a multi-controller approach to manage the complex microbial competition network under these conditions, in essence based on controlling the activity (ON/OFF) and retention (IN/OUT) of the main groups of microbes, promoting specifically aerobic and anoxic ammonium-oxidizing bacteria (AerAOB and AnAOB). The (partial) proliferation of nitrite-oxidizing bacteria (NOB) under mainstream conditions is a typical example imbalancing the AerAOB-AnAOB tandem, resulting in lower nitrogen removal Operational strategies suppressing NOB activity included residual ammonium (>2-4 mg N L^{-1}) and short floccular residence times (2-7 d), combined with intermittent aeration at higher dissolved oxygen (DO) setpoints *e.g.* 1.5 mg O_2 L^{-1} for 0.25-0.5h (Han et al., 2016; Malovanyy et al., 2015; Regmi et al., 2014). The potential AnAOB inhibition by these aeration strategies in i.e. granular or biofilms on carriers, was however not yet addressed. It is unclear to which extent

oxygen hinders PN/A start-up or recovery after a collapse in practice, but an exploratory modeling effort already revealed that full-oxygen penetration can occur in aggregates of 500 µm diameter starting from 1 mg O_2 L^{-1} (See Figure A.1 - C.1).

Oxygen inhibition of AnAOB has been described most extensively for marine systems, as well as for some laboratory freshwater cultures. A wide range of inhibitory values were reported for marine systems, with 50% inhibitory concentrations (IC_{50}) ranging from 0.03 - 0.36 mg O_2 L^{-1} (See Figure D.1) (Babbin et al., 2014; Dalsgaard et al., 2014; Jensen et al., 2008; Kalvelage et al., 2011). The same holds for laboratory freshwater cultures of *Brocadia anammoxidans* or *Kuenenia stuttgartiensis*, with complete inhibition reported at micro-aerobic levels (<0.04-0.12 mg O_2 L^{-1}) (Egli et al., 2001; Oshiki et al., 2015; Strous et al., 1997). In contrast, higher IC_{50} were found for floccular cultures for *Brocadia sinica* (2 mg O_2 L^{-1}) and *Brocadia caroliensis* (3.8 mg O_2 L^{-1}) (Carvajal-Arroyo et al., 2013; Oshiki et al., 2011). This variability in reported DO inhibitory levels can be due to inter-genera differences (Oshiki et al., 2015), potential adaptation towards oxygen stress, protection by oxygen consuming bacteria in small aggregates (Dalsgaard et al., 2014), and testing procedures (Dalsgaard et al., 2014) i.e. mixing, aggregate size, etc. Furthermore, most studies done on fresh-water cultures tested an one-time exposure on anoxically enriched AnAOB, potentially influencing kinetics (Carvajal-Arroyo et al., 2013.; Egli et al., 2001; Lotti et al., 2012; Oshiki et al., 2011). Since AnAOB showed adaptation towards oxygen stress in their transcriptome (Yan et al., 2012), tests with recurring oxygen exposure should be performed with AnAOB to mimic real operation conditions and obtain closer-to application kinetics.

Mathematical models have been widely used to study and optimize the PN/A process under different conditions (Hao et al. 2005, Ni et al. 2014, Terada et al. 2007, Pérez et al. 2014). The oxygen stress on AnAOB was a crucial factor for such modeling efforts, influencing reactor performance e.g. by comparing different aeration patterns (Corbala-Robles et al. 2016). In this case, oxygen inhibition was modeled by an instant recovery Monod inhibition model (Henze et al. 2000). This is in line with the experimental studies so far, where almost all focused-on activity loss during oxygen exposure, which can be described by such model. Yet, only two studies looked at recovery of activity after anoxic conditions were restored (Lotti et al., 2012.; Strous et al., 1997). Both Lotti et al. (2012) and Strous et al. (1997) reported no loss of activity after exposure. As both studies used thick granules with a diameter of 1.1 mm, limited oxygen diffusion through the biofilm could have prevented oxygen inhibition. On the other hand, the low resolution of data, i.e. 6 data points over a period of 2h in the case of Strous et al. (1997), could have disguised short-term recovery effects.

In this study, the effect of DO-pulse concentration and length on AnAOB activity was mapped, by dosing oxygen into an autotrophically fed anammox reactor. Ammonium profiles were measured online and converted to high-resolution AnAOB activities by a newly developed data pipeline. Representative kinetic data were obtained by minimizing diffusional limitations by using flocs ($Ø_{4.3}$ = 168 µm), and by applying recurrent oxygen exposure. As the experimental data did not fit the conventionally used 'instant recovery' Monod model, a new model is proposed based on a more gradual recovery of AnAOB activity. This model was used to assess the long-term impact and implications of oxygen exposure in a AnAOB process model.

2. Material and methods

2.1. Anammox reactor

2.1.1. Inoculum

For the reactor start-up, the goal was to obtain an inoculum rich in AnAOB with minimum diffusion limitations (small particle size). Hereto the cyclone underflow fraction of a sidestream PN/A treatment facility was sampled (WWTP Nieuwveer, Breda, NL). Then, the fraction highest in AnAOB was further selected by sieving this sludge over a 200 µm sieve, assisted by adding tap water. To minimize diffusional limitations, the recovered from the sieve was then blended (± 2 min) in a kitchen blender and sieved again with reactor medium lacking in N-substrate over a 200 µm sieve. The blended, floccular biomass was retained, while unwanted, larger (in)organic particles were removed.

2.1.2. Reactor set-up and SBR operation

The biomass was cultured in a 5.5 L anoxic sequencing batch reactor (SBR) and fed with a synthetic autotrophic medium with ammonium and nitrite as nitrogen sources in a 1/1.3 ratio. The medium was made anoxic through N_2 gas flushing, had a pH of 7.2, and contained per L, 0.5 g of NH_4^+-N as NH_4Cl, 0.65 g of NO_2^--N as $NaNO_2$, 0.5 g $NaHCO_3$, 3.9 g HEPES, 0.1 g $CaCl_2*2H_2O$, 0.2 g $MgSO_4*7H_2O$, 0.06 g $Na_2HPO_4*2H_2O$ and 1 mL of trace elements solutions A and B (Supplemental information E.1). Stirring occurred with an IKA RW20D (IKA, USA). DO levels and temperature were measured online by an Oxymax COS61D sensor with a response time of 1s (Endress and Hauser, CH), whereas pH, ammonium, and potassium were measured by an IseMax CAS40D sensor with response time <2 min (Endress and Hauser, CH). The

signals were sent to a Liquiline CM448 (Endress and Hauser, CH), which transmitted the signals to DaqFactory software (Azeotech, Oregon, USA). This software controlled and monitored the reactor operation and measurements. A typical SBR cycle was as follows. 1.) A new dose of influent (0.23 L over 4 min) was given every time nitrite was depleted, i.e. when ammonium was below a certain residual level and when the rate was below 40 mg N L^{-1} d^{-1}. A residual ammonium level >5 mg N L^{-1} was chosen to ensure that nitrite was always the limiting substrate. 2.) Similarly, 3 additional doses were given, raising the volume of the SBR from 4.25 to 5.17 L. 3.) After nitrite was depleted in the last spike, biomass settled for 30 minutes. 4.) Hereafter, the effluent was pumped out over a period of 7.5 minutes, and the cycle recommenced. The volumetric ammonium removal activity of the reactor determined the influent flow rate fed to the system, resulting in hydraulic retention times varying between 1.7 and 2.5 d over the course of the experiment.

2.1.3. Reactor conditions

The reactor was operated for 120 days, and the reactor conditions were chosen to induce stable and optimal operation, with the added oxygen spikes as only disturbing factor. 1.) The reactor was kept anoxic by N_2-gas flushing (except during an oxygen spike), and the change of headspace volume due to SBR cycling was compensated by a gas bag. 2.) pH was controlled at pH 7.2 by a 0.02 M HCl solution to compensate for the increase in pH from the AnAOB reaction and stripping when flushing with N_2 gas. Under stable operation, the control of pH had a maximum ΔpH = 0.05. No limitation for CO_2 was prevalent, because the reactor was buffered well at pH 7.2 (no large pH fluctuations). 3.) The reactor was located in a temperature-controlled room at 20°C (=no thermostat was used). The temperature was stable during all experiments (avg. standard deviation = 0.1 °C) except for the experiment on day 18 (T = 21.5 ± 0.8), where the measured activity was corrected with a temperature Arrhenius coefficient Θ_T = 1.10 (Lotti et

al., 2014). 4.) Salinity (~43 mM NaCl), ammonium levels (5-40 mg N L^{-1}), nitrite levels (0-35 mg N L^{-1}) and nitrate levels (~100 mg N L^{-1}) were all kept well below reported inhibitory levels for the genus *Brocadia* (Oshiki et al., 2015). 5.) Floccular sludge ($Ø_{4,3}$ = 168±24 µm) and fast stirring (200 rpm) was used to minimize diffusional limitations. Fast stirring also ensured no biofilm growth on the reactor walls. Sludge was regularly taken out of the reactor for batch activity tests, resulting in a stable biomass concentration of 1.95±0.08 g VSS L^{-1} that showed an activity of 1184±188 mg NH_4^+ g VSS^{-1} d^{-1} over the course of the experiments.

2.2. Oxygen response curves in the reactor

2.2.1. Experimental procedure

Two types of oxygen exposure experiments were executed; one in presence and one in absence of nitrite during oxygen exposure. Ammonium was always present during exposure. For the experiments in the presence of nitrite, the oxygen was applied at the start of an SBR cycle after feeding. Oxygen was introduced with a syringe that added a certain volume of air in the bulk liquid. The oxygen level was adjusted manually to the desired level over a period of 2-hours by adding extra air in the headspace of the reactor. After the oxygen exposure period, the reactor was flushed with N_2-gas, to restore anoxic conditions and the recovery of AnAOB activity was monitored. The experiments in absence of nitrite were executed in a similar way, but N sources were supplied manually. Ammonium (~25 mg NH_4^+-N L^{-1}) was supplemented before the oxygen spike, and nitrite (~32.5 mg NO_2^--N L^{-1}) was added when the DO was below <0.02 mg O_2 L^{-1} during flushing. For both sets of experiments, different oxygen concentrations (C) and exposure times (t) were applied (See Table 1).

2.2.2. Data processing: from ammonium concentrations to removal rates

Datasets of the separate experiments were analyzed using Python (PSF, Oregon, USA). Several functionalities were implemented to obtain a reproducible workflow, also conceptually explained in Supplemental Information F.1 and Figure F.2. In short, for each substrate doses in the SBR cycle, the ammonium profile was monitored. These online ammonium measurements were first filtered. Double ammonium values and measurement errors were removed. In a next step, a calculation-window, over which the slopes were calculated was selected manually. This was done to remove the peak of substrate dose at the start and to remove the lower slopes due to nitrite limitation at the end. Within this calculation-window, a smaller Δt value of 10 minutes was chosen to calculate a higher frequency of slopes. From all the calculated slopes, a response curve was constructed. All code written for the data analysis, along with an example Jupyter Notebook and example datasets, are available online: https://zenodo.org/account/settings/github/repository/UGentBiomath/2017_HighResolutionRateCalculation.

2.2.3. Definitions

For interpretation of the response curve, different parameters were defined:

- The activity 'lag phase' was defined as the time before activity starts after oxygen exposure.
- The 'initial recovery' after oxygen inhibition was defined as the first rate calculated after oxygen was depleted.
- The 'recovery time' was calculated as the time between the initial recovery and the first timepoint when full recovery or steady-state was observed, i.e. when the relative %

change in average activity in the actual substrate spike compared to the previous substrate spike was <1%.

- 'Irreversible inhibition' was calculated as the difference between steady-state activity and activity prior to oxygen exposure.

2.3. Mathematical modeling

A simple mathematical model was constructed in Aquasim 2.1g (Reichert, 1998) to conceptually represent the gradual recovery phenomena that were observed in the experiments. The model only included AnAOB biomass at a constant concentration (X_{AnAOB}) during the simulation runs. Because the simulations (and experiments) ran only for 1-2 days, no biomass growth was expected, and was thus not accounted for. Influent ammonium and nitrite concentrations were 50 mg N L^{-1} and 60 mg N L^{-1}, respectively. The model was composed of a conventional Monod-type growth process and a decay process (see Tables G.1 and H.1). To represent a delayed recovery of the AnAOB activity, the growth rate μ_{AnAOB} was modeled as a state variable and was allowed to change depending on the specific conditions. The differential equation (eq. 1) that defined the change of μ_{AnAOB} over time was:

$$\frac{d\mu_{AnAOB}}{dt} = -k_d \cdot \mu_{AnAOB} \cdot \frac{S_O}{S_O+K_O} + \alpha\left(\mu_{m,AnAOB} - \mu_{AnAOB}\right) \cdot \left(\frac{K_O}{K_O+S_O}\right) \quad \text{(eq. 1)}$$

where k_d is the deactivation constant of AnAOB under anoxic conditions (used to set the minimum activity) and α is an adaptation parameter of AnAOB to aerobic conditions. The effect that is introduced by this equation can be linked to the deactivation of enzymes under aerobic conditions which are critical for AnAOB. k_d is representing the deactivation of these enzymes similarly to the model by Kornaros et al. (2010), and α the ability to adapt to environmental

changes (Kornaros et al. 1998). S_O is the oxygen concentration (imported experimental data) and K_O the oxygen inhibition concentration for AnAOB from literature.

To determine the unknown variables k_d and α, the parameter estimation function in Aquasim was used employing the secant method (Reichert, 1998), fitting the experimentally determined relative AnAOB activity to the relative activity calculated by the model. The adapted, 'gradual recovery' Monod-type model, with dynamic μ_{ANAOB}, was compared to the conventional, instant recovery Monod-type model with a constant μ_{ANAOB}.

Model fits were compared based on χ^2, the sum of the squares of the weighted deviations between measurements (Reichert, 1998) and simulated model results (eq. 2). Due to the lack of activity data during the oxygen exposure, only the datapoints after the DO peak (starting with the first activity data point) were used to calculate χ^2.

$$\chi^2(p) = \sum_{i=1}^{n} \left(\frac{y_{data,i} - y_i(p)}{\sigma_{data,i}} \right)^2 \quad \text{(eq. 2)}$$

with $y_{data,i}$ being the i-th measurement, $\sigma_{data,i}$ the standard deviation, $y_i(p)$ the calculated value of the model variable corresponding to the *i-th* measurement and $p = (p_1, \ldots, p_m)$ the model parameters, and n the number of data points.

To extrapolate the results to a process level, the gradual-recovery model was used to test intermittent aeration patterns of 30 min on/off and 180 min on/off at two different DO set-points of 0.2 and 1.2 mg O_2 L^{-1} over a period of 5 days (intermittent aeration until day 4). The parameters α and k_d were both set to a value of 2 for this exercise.

2.4. Oxygen response in batch tests

A batch activity test was executed to determine AnAOB activity after extreme oxygen stress conditions: exposure to 8 mg O_2 L^{-1} for 24h in presence of 40 mg NH_4^+-N L^{-1}. Flocs were taken from the reactor at day 114 and placed in a pH 7.2 corrected medium of 3.87 g HEPES L^{-1}, 0.2 g $CaCl_2x2H_2O$ L^{-1}, 0.1 g $MgSO_4x7H_2O$ L^{-1}, 0.005 g $Na_2HPO_4x2H_2O$-P L^{-1}, 0.5 g $NaHCO_3$ L^{-1}, 40 mg NH_4Cl-N L^{-1} and 1 mL L^{-1} trace elements solutions A and B (Table E.1). The Schott bottles were put on a stirrer and exposed to the air for 24h (=aerobic treatment), reaching 8 mg O_2 L^{-1} within the first hour. The bottles were then flushed with N_2 gas prior to substrate dosing. Control bottles (anoxic control) were not exposed to oxygen, and flushed at the moment when the aerobic exposure time started. 75 mg NH_4Cl-N and 75 mg $NaNO_2$-N L^{-1} were spiked at the beginning of the test. Concentrations of NO_2^-, NO_3^- and NH_4^+ were monitored over time. Volatile and total suspended solids (VSS and TSS) were measured to assess floccular sludge concentration to calculate biomass specific rates as mg N g VSS^{-1} d^{-1}. Each test was performed in triplicate.

2.5. Physicochemical analyses (offline)

Nitrite and nitrate were measured with a 761 Compact IC (Metrohm, CH) and NH_4^+ with the Nesslerization method (Greenberg et al., 1992). To follow up biomass levels, volatile and total suspended solids (VSS and TSS) were measured with Standard Methods 2540D and E (Greenberg et al., 1992). The particle size distribution of the sludge was measured with an EyeTech (Ambivalue, NL). The high-resolution B&W CCD video camera determined the volume weighed average particle diameter in a ACM-101 magnetic stirring cell with the following settings: sample dilution 1:10, camera lens DW (range 10-600 µm), and setup = sludge DW A101.

2.6. Molecular biomass analyses

Total genomic DNA was extracted from the biomass samples using the Fast DNA Spin kit for soil (MP Biomedicals, US) according to a modified manufacturer's protocol. The quality of the DNA was checked using gel electrophoresis, and the concentration was measured using a QUBIT (Thermo Fisher, US). Using the 16S Ion Metagenomics Kit ™ and Ion Xpress Plus Fragment Library Kit ™ (Thermo Fisher, US), V3-V4 16S rRNA hypervariable region amplicon library was generated, and each sample was tagged using Ion Xpress Barcode Adapters 1–16 ™ (Thermo Fisher, US), according to the manufacturer's protocol. Each sample was adjusted to a concentration of 10 picomolar. All samples were pooled in equal volume and processed with One-Touch 2 and One-Touch ES systems (Thermo Fisher, US) according to the manufacturer's instructions. Sequencing was performed on a Ion Torrent (ION Torrent Ion S5) using the 200-bp kit and the 520 chip. Base calling and run demultiplexing were conducted by Torrent Suite version 4.4.2 (Thermo Fisher, US) with default parameters. The Ion reporter software was used for, (1) separating sequences based on their respective targeted regions; (2) then picking OTU (operational taxonomical unit) with its default settings. Overall, the de novo clustering of OTUs was done with 97% identity, corresponding to species level. The sequences were then classified based on the taxonomy in the Greengenes database (97% confidence threshold, version 13.5 May 2013) (McDonald et al., 2012). The sequencing data was analyzed in R, using ggplot2 (v0.9.3.1), to determine the community composition of the biomass in the reactor.

3. Results

3.1. Microbial community enriched in *Ca. Brocadia*

Over the experimental period, the reactor community was enriched in one AnAOB OTU of the genus *Ca. Brocadia* from 64% (day 38) to 75% (day 106), based on 16S rDNA amplicon sequencing (See Figure I.1 for more detailed community analysis). As this AnAOB is commonly encountered in engineered systems, it is anticipated that its response behavior to oxygen is applicable to PN/A applications (Oshiki et al., 2015).

3.2. Experimental oxygen response curves

AnAOB responded differently towards tested combinations of oxygen concentrations, exposure times and presence or absence of nitrite. An overview of the experiments is given in Table 1, while Figure 1 depicts typical activity curves including modeling efforts. The AnAOB response curve consisted of the following parts which will be described below: AnAOB activity prior and during exposure, an eventual activity lag phase, initial recovery after exposure, and gradual recovery with or without irreversible inhibition.

3.2.1. AnAOB activity in presence of O_2

During oxygen exposure, no ammonium was consumed, and AnAOB activity was only regained when oxygen concentrations were below micro-aerobic conditions <0.02 mg O_2 L^{-1} (Figure 1, Panel C.2 and D.2), indicating a direct and high intolerance to oxygen.

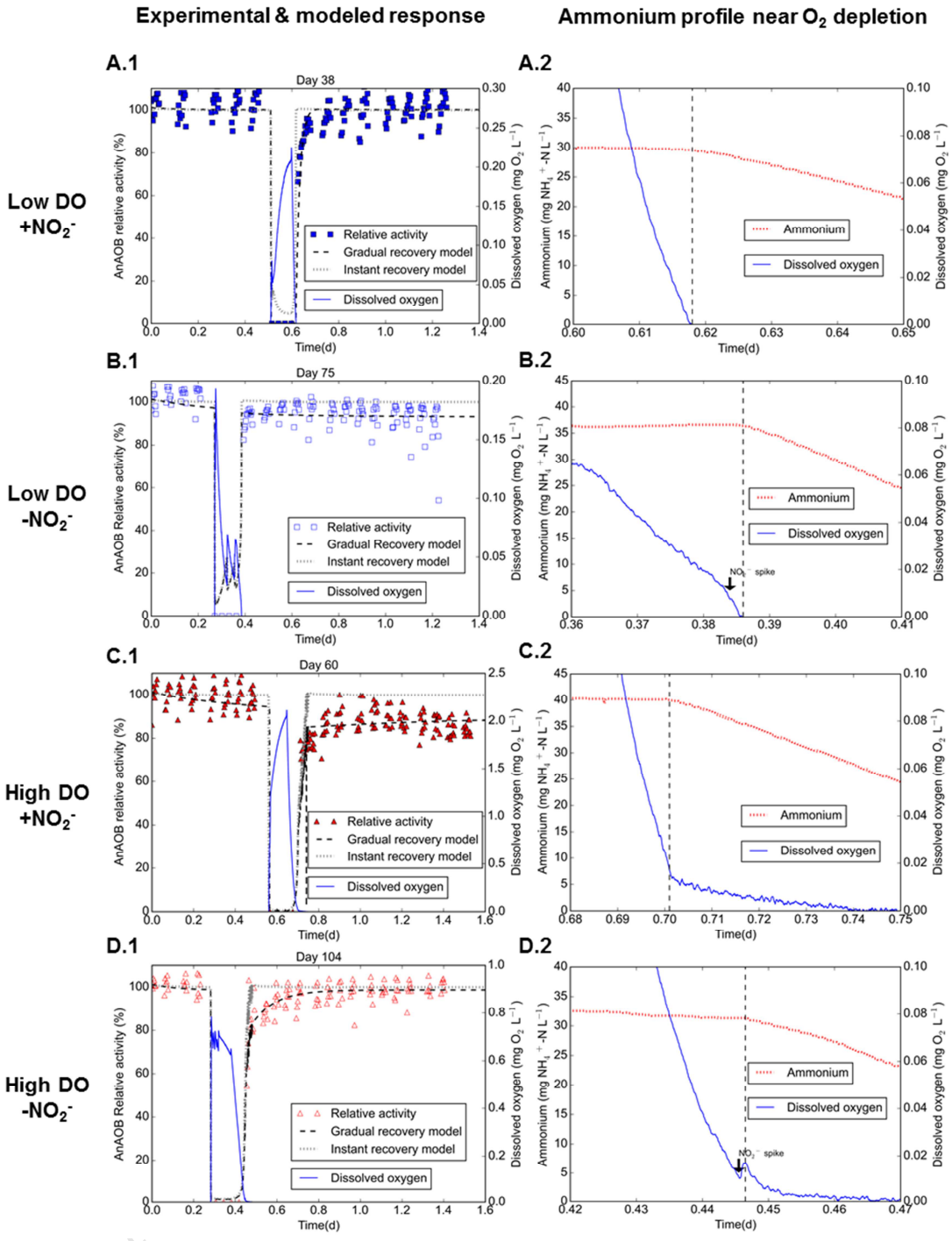

Figure 1. Experimental and modelled response of AnAOB to oxygen exposure in the reactor. Conditions during exposure: low DO (blue squares), high DO (red triangle), subsequently with nitrite (filled) or without nitrite (empty). Ammonium was always present. The left-side graphs show the experimental data compared to an instant recovery Monod model and the newly developed gradual recovery Monod model. The right-side graphs indicate AnAOB activity at micro-aerobic levels. The vertical dashed line represents the moment when ammonium starts to deplete.

3.2.2. AnAOB activity lag phase after oxygen inhibition

After oxygen disappearance, AnAOB reversibly and immediately reinitiated activity to 55-80% of the pre-exposure activity, depending on the conditions during exposure. This drop of initial recovery after oxygen inhibition was not due to substrate (ammonium and nitrite) starvation during exposure, because longer anoxic periods without substrate did not result in activity loss. In an *ex-situ* batch test, the effect of longer oxygen exposure (24h) at a higher oxygen concentration (8 mg O_2 L^{-1}) was tested (Figure 2). Activity could be detected only after a 5h lag phase and it increased gradually from 10% to 91% of the initial activity after 26h under anoxic conditions.

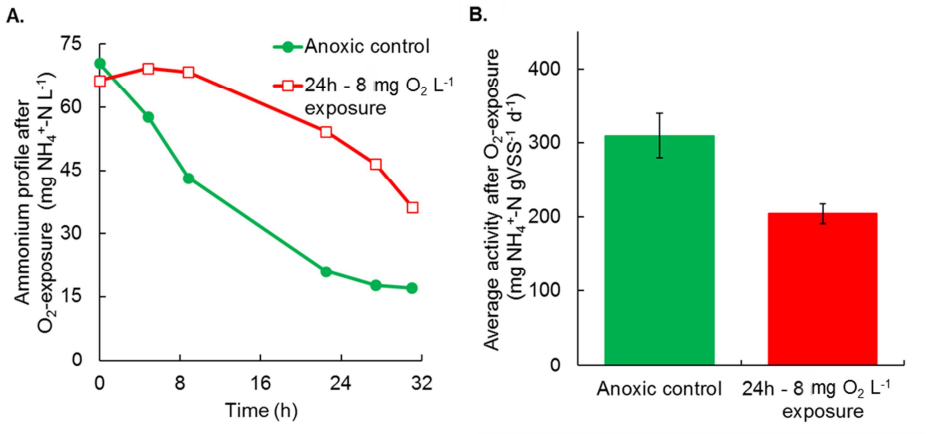

Figure 2. AnAOB recovery after exposure to 8 mg O_2 L^{-1} for 24h with 40 mg NH_4-N L^{-1}, in the absence of nitrite. Ammonium (35 mg N L^{-1}) and nitrite (75 mg N L^{-1}) were dosed after oxygen exposure. Panel A depicts a typical measured ammonium profile after exposure, compared to an anoxically kept control, while Panel B shows the resulting sludge-specific activity after exposure (average ± standard deviation).

3.2.3. Initial recovery after oxygen inhibition

For the *in-situ* reactor tests, initial recovery after oxygen inhibition decreased from 81±3 % to 74±5% when AnAOB were exposed to higher compared to lower oxygen concentrations in absence of nitrite, on avg. 0.47±0.08 vs. 0.08±0.04 mg O_2 L^{-1} (Figure 3). This increased drop in initial recovery could also be due to longer exposure times for the high DO-setpoint (Figure J.1), which were on avg. 3.7±0.3 h vs. 2.8±0.2 h for the low DO-setpoint. A lower initial recovery after oxygen inhibition was also recorded when AnAOB were exposed to 0.5±0.2 mg O_2 L^{-1} for 8.7h in the presence of nitrite, with a gradual recovery from 58% to full recovery after 37h (Day 18).

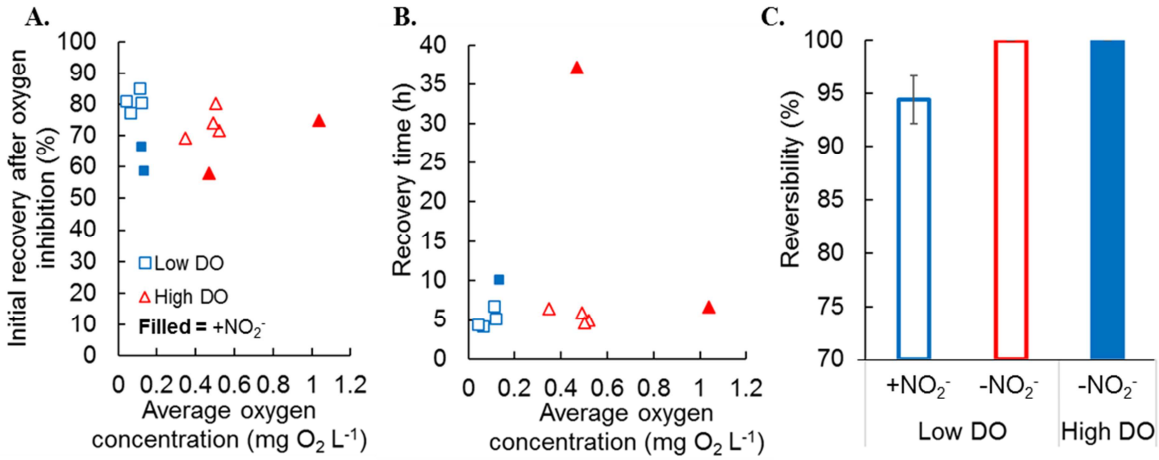

Figure 3. Depicting the calculated kinetic parameters from the experimental reactor data. A.) Measured initial recovery as a function of the oxygen exposure concentration, B.) time to reach steady state activity after exposure (= recovery time) and C.) reversibility of activity after exposure. Plotted data can be found in Table K.1.

3.2.4. Gradual recovery

After exposure, AnAOB gradually recovered towards a steady-state activity. This recovery time until steady state was similar for the low and high DO-setpoint, and in the range of 4.2-6.8h, with

on avg. 6.3±0.9 h. The recovery time also did not show any correlation with the concentration (C) (Figure J.1), exposure time (t) (Figure J.1), integrated Cxt (Figure J.1) or initial recovery after oxygen inhibition. AnAOB did not always fully recover (see Figure 2, Panel C and Figure 1, Panel B and C), and consistent irreversible loss of activity of about 5% was seen when the biomass was exposed to low oxygen setpoints of on avg. 0.06-0.12 mg O_2 L^{-1} in absence of nitrite. A short 4h exposure with a high DO setpoint of on avg. 1 mg O_2 L^{-1} and in the presence of nitrite also led to more severe irreversible loss of activity of about 9% (Figure 1, Panel C). Conversely, the short-term (~3h) and long term (~8h) exposures at DO setpoints in a range of on avg. 0.12- 0.5 mg O_2 L^{-1} with nitrite, as well as the higher DO setpoints of on avg. 0.35-0.52 mg O_2 L^{-1} in absence of nitrite, did not reveal any irreversible inhibition. This indicates that the complex interplay of oxidative and nitrosative (O_2 + N-species) conditions, combined with substrate presence might regulate how AnAOB cope with oxidative and nitrosative stress.

3.3. Modeling gradual recovery after oxygen inhibition

A gradual-recovery model was constructed to describe the gradual recovery after oxygen inhibition. A comparison with the classical instant recovery model (Figure 1 and Table 1) revealed a considerably improved fit of the gradual-recovery model to the data than the instant recovery model, evident from the 2 – 4-fold lower χ^2. The newly developed gradual-recovery model included a dynamic growth rate to simulate the delay in the recovery of the AnAOB activity (Figure 1).

The automated fitting produced sometimes large variations and/or standard errors for the parameters α and kd. One reason is the high fluctuation of the measured activities during one

SBR cycle of up to ±10%. Another reason is the lack of data for the AnAOB activity during oxygen exposure. To more accurately determine both parameters, more data during initial oxygen exposure and shortly after oxygen depletion is necessary. Especially kd is highly influenced by the slope of loss and regain of the activity, and the data does not allow for a highly accurate parameter estimation (also visible from the standard deviations of kd). Since kd represents the deactivation of the AnAOB activity due to the oxygen, higher kd values are required for bringing down the activity to zero during oxygen exposure. The parameter α mainly formed the shape of the activity curve during recovery and with higher α values the recovery became faster (Table 1).

Process modeling was further used to estimate the impact of the newly observed oxygen response on a PN/A. This implied evaluating the impact of longer phases of intermittent aeration on the effluent composition of a continuously operated PN/A reactor, with simulations run over 5 days employing different aeration patterns (see M&M). Figure 4 summarizes the results of these simulations, which were evaluated based on the nitrogen species in the effluent exemplarily plotting the ammonium concentration. It was evident that the ammonium concentrations in the effluent as predicted by the gradual-recovery model were higher than the ones predicted by the instant recovery model. From the different conditions tested, a less frequent oxygen alteration (180/180 on/off) rather than a higher oxygen level (1.2 vs 0.2 mg O_2 L^{-1}) yielded high peak ammonium concentrations earlier on. These effects were caused by the decrease in the growth rate in the gradual-recovery model (Figure 4, left row) due to the imposed oxygen peaks. **This decrease in growth rate is influenced by α and k_d (which were set to 2 in this example), leading to more severe effects for lower α values and ratios of α / k_d of < 1.**

394

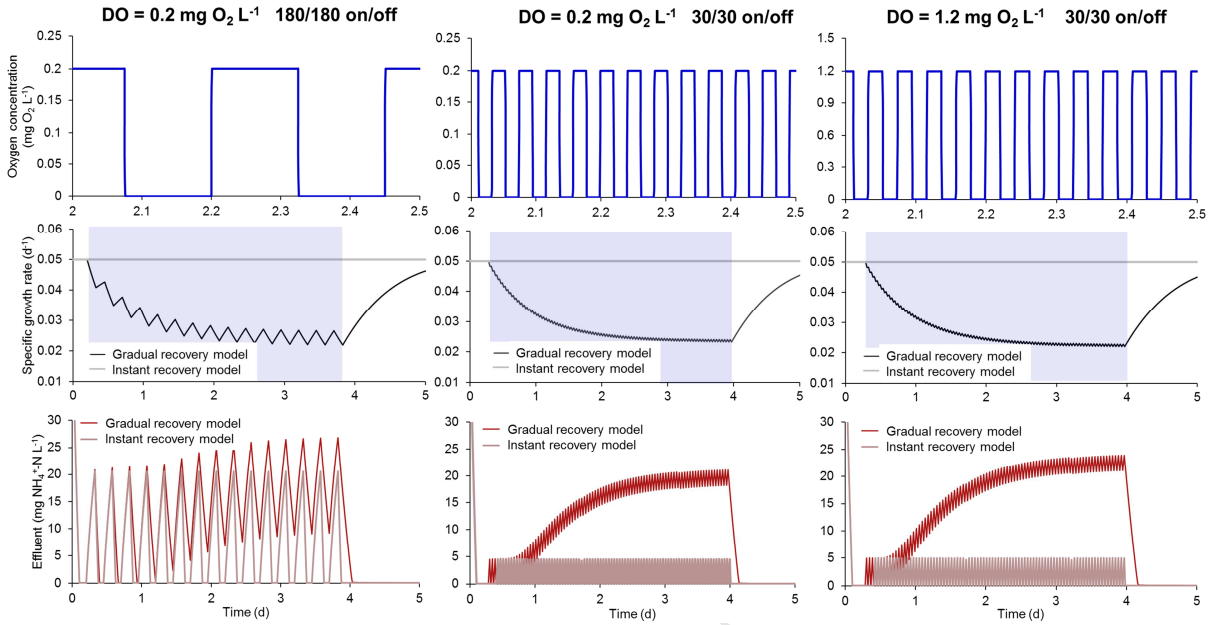

395

396 **Figure 4.** Results of the simulation runs over 5 days employing different intermittent aeration patterns.
397 First row: section of the dissolved oxygen (DO) pattern; second row: growth rate (μ) for the instant
398 recovery Monod model (constant, instant recovery) and the gradual recovery Monod model (dynamic,
399 gradual recovery) and; third row: ammonium effluent concentrations of both models.

4. Discussion

4.1. AnAOB inhibition by oxygen

4.1.1. AnAOB gradual recovery after oxygen inhibition

To our knowledge this is the first report showing at high temporal resolution how AnAOB activity is affected by oxygen exposure. AnAOB were completely inhibited by oxygen, and after short exposure resumed activity directly, with a gradual recovery until reversible activity was overcome. Other anoxic/anaerobic bioconversions, for instance by sulfate reducing bacteria or denitrifying bacteria, which similarly to AnAOB rely on substrates derived from oxidative and reducing conditions at oxic and anoxic/anaerobic interfaces, responded kinetically similarly after oxygen exposure (Dolla et al., 2006; Fareleira et al., 2003; Kornaros & Lyberatos, 1998). AnAOB and other microbes living under recurrent oxygen exposure thus adapted towards these conditions, with production of anti-oxidative enzymes and recovery of activity after exposure, which cannot be explained by growth (Dalsgaard et al., 2014; Yan et al., 2012).

The measured kinetic response is most likely overlooked so far because most studies investigated activity only during exposure. In the scarce cases studying also recovery, the outcome might have been biased due to lower data resolution after exposure, *i.e.* 4-6 datapoints over a course of 2-6 h (Dalsgaard et al., 2014.; Strous et al., 1997) or aggregate size (Lotti et al., 2012; Strous et al., 1997). For example, Strous et al. (1997) reported no influence on biomass specific activity rates when a granular biomass *(Brocadia)* was repeatedly exposed for 20 days to 2h aerobic and anoxic conditions. Similarly, Lotti et al. (2012) reported no loss in activity after an extreme oxygen exposure of 24h and 5 mg O_2 L^{-1} for granular biomass (Ø=1.1 mm). In both

422 cases, diffusional limitations could have underestimated initial biomass specific activities, and
423 consequentially inhibition could be masked by this underestimation.

424

425 4.1.2. Factors impacting initial recovery after oxygen inhibition

426 With the current dataset, it was not feasible to deduct whether the oxygen concentration (Figure
427 2) or exposure time (Figure J.1) had a larger influence on the initial recovery, as higher oxygen
428 concentrations also had longer exposure times. It was hypothesized that 'concentration times
429 exposure time' (Integrated Cxt, Figure J.1) steered the AnAOB response, but Spearman rank
430 correlation analysis did not yield any correlation. From the gradual-recovery model, the
431 exposure time had a higher influence than the concentration, while other factors like adaptation
432 and nitrite presence during exposure might differentiate the response and thus fitted kinetic
433 parameters. Both aspects require further experimental research to elucidate the exact factors
434 determining initial recovery after oxygen inhibition.

435

436 4.1.3. Novel experimental procedure and impact on measured kinetics

437 In this study, AnAOB responded very sensitive towards oxygen, with an observed IC_{100} 0.02 mg
438 O_2 L^{-1} or below. This showed that diffusional limitations in rather large flocs of ~200 µm or
439 oxygen consumption by putative heterotrophs in the AnAOB satellite community did not shield
440 AnAOB from oxygen. AnAOB sensitivity towards oxygen was comparable with some freshwater
441 AnAOB, *Brocadia sp*. and *Kuenenia stuttgartiensis*, which were for 100% inhibited at micro-
442 aerobic conditions of <0.04 and <0.12 mg O_2 L^{-1} respectively (Egli et al., 2001; Strous et al.,
443 1997). In contrast, two *Brocadia*-enriched floccular sludge types were very tolerant towards
444 oxygen exposure, with IC_{50} values of 2 and 3.8 mg O_2 L^{-1} respectively, which cannot be

445 explained when compared to our or other studies (See Figure D.1) (Carvajal-Arroyo et al., 2003;
446 Oshiki et al., 2011). Also, for marine AnAOB, higher IC_{100} values between 0.09 and 0.64 mg O_2
447 L^{-1} were reported (Babbin et al., 2014; Dalsgaard et al., 2014; Jensen et al., 2008; Kalvelage et
448 al., 2011). For the latter, the difference between measured sensitivities was hypothesized to
449 come from either different testing conditions, *i.e*. absence of mixing or presence in aggregates,
450 shielding AnAOB (partially) from oxygen, or from more adapted AnAOB due to presence in
451 oxygen minimum zones (Dalsgaard et al., 2014). As in our testing conditions AnAOB were
452 repeatedly exposed to oxygen with low diffusional limitations, the obtained data probably
453 resembled intrinsic and more adapted kinetics. The newly developed methodology, which
454 obtained high-resolution data processed by a data-pipeline, is therefore highly suitable for
455 studying kinetic responses of stressors and inhibitors on AnAOB.

456

457 ## 4.2. Modeling AnAOB inhibition by oxygen

458 In mathematical modeling, oxygen inhibition of AnAOB has typically been modelled by an
459 instant-recovery Monod model with an inhibition constant $K_{O,AnAOB}$ of 0.01 mg L^{-1} (based on
460 Strous et al., 1998). With this kinetic constant, 10% AnAOB activity is expected at 0.1 mg O_2 L^{-1},
461 which overestimated the expected activity of AnAOB during oxygen exposure in our
462 experiments (See Figure 1). Further fine-tuning of this kinetic constant is thus necessary. After
463 oxygen exposure, AnAOB directly resumed activity only in a range of 30-80% of the initial
464 activity. This direct recovery of activity was conventionally reported and perceived as reversible
465 activity of AnAOB without any activity loss (Dalsgaard et al., 2014; Egli et al., 2001; Lotti et al.,
466 2012; Strous et al., 1997). Instant-recovery models therefore do not account for a delay in
467 recovery to less than 100%, while the newly developed gradual-recovery model describes this
468 more accurately. Gradual recovery has been previously modelled for several other nitrogen bio-

conversions. Alex et al. (2009) and Casasus et al. (2005) introduced an enzyme as additional state variable, and processes for its activation and deactivation to simulate bacterial lag phases for nitrification (Alex et al., 2009) and denitrification (Casasus et al., 2005). Identically to our approach, the NOB lag phase after anoxic phases (Kornaros et al. 2010) was successfully modeled with the growth rate as dynamic variable thus influencing the maximum specific growth rate. The latter enabled to exploit these lag phenomena to optimize NOB suppression in their reactors. These examples show that incorporating additional equations may lead to more accurate models and further insights on how to optimally operate mainstream PN/A. Additional research is needed, however, due to the limited amount of data, especially during oxygen exposure, to accurately estimate the newly introduced parameters, α and k_d, independently. Furthermore, other effects like exposure time, oxidative stress conditions and adaptation could also impact the modeled parameters, and should be taken into account in further modeling exercises.

4.3. Long-term recurrent exposure: exploratory simulations

From a modelling perspective, the exposure time is the critical parameter when looking at the implications on effluent quality (Figure. 4). The simplified model showed that a delay in the recovery of full activity will potentially lead to a decrease of the overall turnover capacity of the system, which is reflected in the effluent concentration (exemplified by ammonium). An instant-recovery model, where the activity is back to 100% right after oxygen depletion, does not capture such a delay and will therefore not account for any impact this had on the reactor performance. The model suggested that longer anoxic periods in combination with short intense aeration intervals might be the strategy of choice. However, the model in its present form does not account for other effects, that might influence recovery, such as adaptation (Yan et al.,

493 2012), niche differentiation (Oshiki et al., 2015), aggregate morphology, or nitrite availability,
494 which also seemed relevant from the experimental observations.

495

496 In practice, also aerobic processes and mass transfer limitations partially shield AnAOB in
497 biofilms from oxygen exposure. For this reason, increased AnAOB resilience was reported in
498 biofilm systems compared to flocs, e.g. lower nitrite build-up was detected when nitrification
499 (and thus oxygen shielding) failed due to sudden or long-term disturbances in temperature
500 drops (Gilbert et al., 2016.; Wells et al., 2017). However, completely anoxic conditions might be
501 hard to achieve, and will also depend on the height of the oxygen peaks (See Figure in B.1).
502 AnAOB recovery from oxygen inhibition will thus always be present in PN/A reactors, and
503 studies on long-term repeated exposure are warranted to achieve the process intensification,
504 i.e. maximize nitrogen removal rates and efficiencies.

505

5. Conclusions

AnAOB reside mostly in proximity of oxygen in wastewater treatment processes such as PN/A, possibly experiencing repeated inhibition. Nonetheless, it was not well understood how AnAOB activity is affected by oxygen stress. A newly developed methodology, which combined high temporal resolution measurements with a fit-for-use data-pipeline enabled to study this, and corroborate the findings with a newly developed mathematical model.

1. AnAOB showed no activity during exposure (<0.02 mg O_2 L^{-1}). Due to oxygen inhibition, AnAOB lost activity compared to pre-exposure rates. This initial loss in activity was followed by a gradual (partial) recovery of activity, dependent on the oxidative (or nitrosative) stress conditions perceived during oxygen exposure.
2. The initial recovery after oxygen inhibition was slower when exposed towards higher dissolved oxygen concentrations and contact times.
3. Exposure to low oxygen concentrations of 0.05-0.2 mg O_2 L^{-1} did not result in full recovery (~95%).
4. A new gradual-recovery Monod model described the gradual recovery more accurately than the current instant-recovery model.
5. Long-term simulated exposure with intermittent aeration and the gradual-recovery model led to reduced AnAOB growth rates compared to an instant recovery model. Considering oxygen inhibition on AnAOB can thus be an important factor to optimize aeration patterns in single-stage PN/A reactors, allowing to maximize nitrogen removal rates and efficiencies.

6. Acknowledgements

D.S. was supported by a PhD grant from the Institute for the Promotion of Innovation by Science and Technology in Flanders (IWT-Vlaanderen, SB-131769). This project was also supported by the Dutch Ministery of Economic Affairs based on the 'Regeling Nationale EZ-subsidies & Hernieuwbare Energie'.

7. References

Alex, J., Holm, N. C., & Rönner-Holm, S. G. E. (2009). Lag phase, dynamic alpha factor and ammonium adsorption behaviour: introduction of special activated sludge characteristics in the ASM3+ EAWAG-BioP-model. *Water Science and Technology*, 59(1), 133-140.

Babbin, A. R., Keil, R. G., Devol, A. H., & Ward, B. B. (2014). Organic matter stoichiometry, flux, and oxygen control nitrogen loss in the ocean. *Science*, *344*(6182), 406-408.

Agrawal, S., Seuntjens, D., De Cocker, P., Lackner, S., & Vlaeminck, S. E. (2018). Success of mainstream partial nitritation/anammox demands integration of engineering, microbiome and modeling insights. Current opinion in biotechnology, 50, 214-221.

Carvajal-Arroyo, J. M., Sun, W., Sierra-Alvarez, R., & Field, J. A. (2013). Inhibition of anaerobic ammonium oxidizing (anammox) enrichment cultures by substrates, metabolites and common wastewater constituents. *Chemosphere*, *91*(1), 22-27.

Casasús, A. I., Hamilton, R. K., Svoronos, S. A., & Koopman, B. (2005). A simple model for diauxic growth of denitrifying bacteria. *Water Research*, *39*, 1914–20.

Corbalá-Robles, L., Picioreanu, C., van Loosdrecht, M. C., & Pérez, J. (2016). Analysing the effects of the aeration pattern and residual ammonium concentration in a partial nitritation-anammox process. *Environmental Technology*, *37*, 694–702.

Dalsgaard, T., Stewart, F. J., Thamdrup, B., De Brabandere, L., Revsbech, N. P., Ulloa, O., ... & DeLong, E. F. (2014). Oxygen at nanomolar levels reversibly suppresses process rates and gene expression in anammox and denitrification in the oxygen minimum zone off northern Chile. *MBio*, *5*(6), e01966-14.

Dolla, A., Fournier, M., & Dermoun, Z. (2006). Oxygen defense in sulfate-reducing bacteria. *Journal of Biotechnology*, *126*, 87–100.

Egli, K., Fanger, U., Alvarez, P. J., Siegrist, H., Meer, J. R., & Zehnder, A. J. (2001). Enrichment and characterization of an anammox bacterium from a rotating biological contactor treating ammonium-rich leachate. *Archives of Microbiology*, *175*, 198–207.

Fareleira, P., Santos, B. S., António, C., Moradas-Ferreira, P., LeGall, J., Xavier, A. V., & Santos, H. (2003). Response of a strict anaerobe to oxygen: survival strategies in Desulfovibrio gigas. *Microbiology*, *149*(6), 1513-1522.

Gilbert, E. M., Agrawal, S., Schwartz, T., Horn, H., & Lackner, S. (2015). Comparing different reactor configurations for partial nitritation/anammox at low temperatures. *Water research*, *81*, 92-100.

Greenberg, A., Clesceri, L., & Eaton, A. (1992). *Standard Methods for the Examination of Water and Wastewater*. Washington DC: American Public Health Association.

Han, M., Vlaeminck, S. E., Al-Omari, A., Wett, B., Bott, C., Murthy, S., & De Clippeleir, H. (2016). Uncoupling the solids retention times of flocs and granules in mainstream deammonification: A screen as effective out-selection tool for nitrite oxidizing bacteria. *Bioresource Technology*, *221*, 195–204.

Hao, X. D., Cao, X. Q., Picioreanu, C., & Van Loosdrecht, M. C. M. (2005). Model-based evaluation of oxygen consumption in a partial nitrification–anammox biofilm process. *Water science and technology*, *52*(7), 155-160.

Henze, Gujer, Mino, & Loosdrecht, M. (2000). Activated sludge models ASM1, ASM2, ASM2d and ASM3.

Jensen, M. M., Kuypers, M. M., Gaute, L., & Thamdrup, B. (2008). Rates and regulation of anaerobic ammonium oxidation and denitrification in the Black Sea. *Limnology and Oceanography*, *53*(1), 23-36.

Kalvelage, T., Jensen, M. M., Contreras, S., Revsbech, N. P., Lam, P., Günter, M., ... & Kuypers, M. M. (2011). Oxygen sensitivity of anammox and coupled N-cycle processes in oxygen minimum zones. *PloS one*, *6*(12), e29299.

Kornaros, M. S. N. D., Dokianakis, S. N., & Lyberatos, G. (2010). Partial nitrification/denitrification can be attributed to the slow response of nitrite oxidizing bacteria to periodic anoxic disturbances. *Environmental science & technology*, *44*(19), 7245-7253.

Kornaros, M, & Lyberatos, G. (1998). Kinetic modelling of Pseudomonas denitrificans growth and denitrification under aerobic, anoxic and transient operating conditions. *Water Research*, *32*, 1912–1922.

Lackner, S., Gilbert, E. M., Vlaeminck, S. E., Joss, A., Horn, H., & van Loosdrecht, M. C. (1901). Full-scale partial nitritation/anammox experiences – An application survey. *Water Research*, *55*, 292–303.

Lotti, T., Van der Star, W. R. L., Kleerebezem, R., Lubello, C., & Van Loosdrecht, M. C. M. (2012). The effect of nitrite inhibition on the anammox process. *Water research*, *46*(8), 2559-2569.

Lotti, T., Kleerebezem, R., Lubello, C., & Van Loosdrecht, M. C. M. (2014). Physiological and kinetic characterization of a suspended cell anammox culture. *Water research*, *60*, 1-14.

Malovanyy, A., Trela, J., & Plaza, E. (2015). Mainstream wastewater treatment in integrated fixed film activated sludge (IFAS) reactor by partial nitritation/anammox process. *Bioresource Technology*, *198*, 478–487.

McDonald, D., Price, M. N., Goodrich, J., Nawrocki, E. P., DeSantis, T. Z., Probst, A., … Hugenholtz, P. (2012). An improved Greengenes taxonomy with explicit ranks for ecological and evolutionary analyses of bacteria and archaea. *The ISME Journal*, *6*, 610.

Ni, B. J., Joss, A., & Yuan, Z. (2014). Modeling nitrogen removal with partial nitritation and anammox in one floc-based sequencing batch reactor. *Water research*, *67*, 321-329.

631 Oshiki, M., Satoh, H., & Okabe, S. (2015). Ecology and physiology of anaerobic ammonium
632 oxidizing bacteria. *Environmental Microbiology*, *18*, 2784–2796.
633
634 Oshiki, M., Shimokawa, M., Fujii, N., Satoh, H., & Okabe, S. (2011). Physiological
635 characteristics of the anaerobic ammonium-oxidizing bacterium 'Candidatus Brocadia sinica'.
636 *Microbiology*, *157*, 1706–1713.
637
638 Regmi, P., Miller, M. W., Holgate, B., Bunce, R., Park, H., Chandran, K., ... & Bott, C. B. (2014).
639 Control of aeration, aerobic SRT and COD input for mainstream nitritation/denitritation. *Water*
640 *research*, *57*, 162-171.
641
642 Reichert, P. (1998). AQUASIM 2.0–user manual. *Swiss Federal Institute for Environmental*
643 *Science and Technology.* Dubendorf, Switzerland.
644
645 Strous, M., Heijnen, J. J., Kuenen, J. G., & Jetten, M. S. M. (1998). The sequencing batch
646 reactor as a powerful tool for the study of slowly growing anaerobic ammonium-oxidizing
647 microorganisms. *Applied microbiology and biotechnology*, *50*(5), 589-596.
648
649 Strous, M., Van Gerven, E., Kuenen, J. G., & Jetten, M. (1997). Effects of aerobic and
650 microaerobic conditions on anaerobic ammonium-oxidizing (anammox) sludge. *Applied and*
651 *environmental microbiology*, *63*(6), 2446-2448.
652
653 Terada, A., Lackner, S., Tsuneda, S., & Smets, B. F. (2007). Redox-stratification controlled
654 biofilm (ReSCoBi) for completely autotrophic nitrogen removal: The effect of co-versus counter-
655 diffusion on reactor performance. *Biotechnology and Bioengineering*, *97*(1), 40-51.
656
657 Verstraete, W., & Vlaeminck, S. E. (2011). ZeroWasteWater: short-cycling of wastewater
658 resources for sustainable cities of the future. *International Journal of Sustainable Development*
659 *& World Ecology*, *18*, 253–264.
660
661 Wells, G. F., Shi, Y., Laureni, M., Rosenthal, A., Szivák, I., Weissbrodt, D. G., ... & Morgenroth,
662 E. (2017). Comparing the Resistance, Resilience, and Stability of Replicate Moving Bed Biofilm
663 and Suspended Growth Combined Nitritation–Anammox Reactors. *Environ. Sci. Technol*, *51*(9),
664 5108-5117.
665
666 Yan, J., Haaijer, S., Op den Camp, H. J., Niftrik, L., Stahl, D. A., Könneke, M., ... & Jetten, M. S.
667 (2012). Mimicking the oxygen minimum zones: stimulating interaction of aerobic archaeal and
668 anaerobic bacterial ammonia oxidizers in a laboratory-scale model system. *Environmental*
669 *microbiology*, *14*(12), 3146-3158.
670
671

672

Table 1. Overview of reactor experiments executed with low dissolved oxygen (DO) (blue) and high DO (red). Table shows DO exposure concentrations (C), times (t) and integrated exposure (Cxt), along with the parameters obtained from fitting the gradual-recovery model. For both models, i.e. conventional Monod with instant recovery and adapted Monod with gradual recovery, the estimated **χ2** values are given. The lower, the better a fitted model represents the experimental data. Response curves of the days highlighted in bold are shown in detail in Figure 1. **n° = replicate number.**

		Day	n°	DO concentration C		Exposure time t	Integrated exposure Cxt	Gradual-recovery model kinetic parameters		Estimated fit (χ2)	
				Average (mg O_2 L^{-1})	Peak Height (mg O_2 L^{-1})	(h)	(mg O_2 L^{-1} h)	α	k_d	Instant recovery model	Gradual recovery model
Low DO	+ NO_2^- ■	**38**	(1/2)	0.12±0.07	0.23	2.64	0.014	63.7±2.74	2937±4217	11378	5832
		40	(2/2)	0.13±0.06	0.23	2.56	0.014	71.91±5.49	15686±1323	16712	7907
	- NO_2^- □	67	(1/4)	0.06±0.06	0.27	2.88	0.007	2.56±1.02	1.34±0.56	10295	1292
		75	(2/4)	0.06±0.04	0.19	2.64	0.007	1.95±0.72	0.15±0.33	10025	5345
		81	(3/4)	0.12±0.09	0.38	2.64	0.012	4.81±0.92	1.19±0.37	6721	2809
		82	(4/4)	0.12±0.08	0.35	3.12	0.015	4.56±0.71	0.98±0.19	5528	1853
High DO	+ NO_2^- ▲	18	(1/1)	0.47±0.21	0.75	8.71	0.177	9.20±0.43	10131±6771	48482	7281
		60	(1/1)	1.04±0.8	2.11	4.08	0.071	1.30±0.21	0.58±0.13	31000	10080
	- NO_2^- △	85	(1/4)	0.52±0.26	0.75	3.29	0.056	60.5±52.4	6.03±458	9501	7438
		98	(2/4)	0.35±0.24	0.81	3.89	0.088	55.24±7.5	21.95±10.8	10315	4040
		104	(3/4)	0.49±0.24	0.78	4.08	0.088	8.79±1.23	1.42±0.21	723	2208
		106	(4/4)	0.50±0.30	0.84	3.84	0.014	6.94±3.38	0.16±0.32	17054	16274

Highlights

1. During oxygen exposure, anammox bacteria (AnAOB) showed no activity
2. Interestingly, the AnAOB activity recovered only gradually after oxygen exposure
3. The proposed model fitted the data better than the conventionally used model
4. The recovery impacts achievable removal rates for partial nitritation/anammox